JOURNAL OF APPLIED ELECTROCHEMISTRY **27** (1997) 550–557

Electrochemical study of the corrosion behaviour of copper surfaces modified by nitrogen ion implantation

A. JIMENEZ-MORALES
Escuela Politécnica Superior. Universidad Carlos III de Madrid, 28911 Leganés, Spain

J. C. GALVAN
Instituto de Ciencia de Materiales de Madrid (CSIC), Cantoblanco, 28049 Madrid, Spain

R. RODRIGUEZ
Asociación de la Industria Navarra (AIN), E-31191-Cordovilla, Pamplona, Spain

J. J. DE DAMBORENEA*
Centro Nacional de Investigaciones Matalúrgicas (CSIC), Avda. Gregorio del Amo, 8. E-28040 Madrid, Spain

Received 30 May 1995; revised 8 October 1996

Electrochemical impedance spectroscopy (EIS) and d.c polarization resistance measurements (R_p) were used to study the corrosion resistance of surface layers produced by nitrogen ion implantation into copper substrates. Ion implantation was carried out using a Wickham ion beam generator, applying an acceleration voltage of 100 keV, a mean current of 0.40 mA and a nitrogen dosage of 4×10^{17} ions cm^{-2}. Surface analyses were made by Auger electron spectroscopy (AES). Electrochemical measurements (EIS and R_p) performed in a 0.6 M sodium chloride solution show nitrogen-implanted specimens have greater a.c. and d.c. apparent polarization resistance than nonimplanted specimens. The results obtained with electrochemical measurements indicate that nitrogen ion implantation in copper forms a protective surface layer which improves the corrosion resistance of the pristine material, a feature of great interest for the design of new contact materials for the electricity and electronic industries.

1. Introduction

Ion implantation is one of the surface modification techniques most widely developed in recent years. The surface to be treated is bombarded by high energy ions (50–200 keV) and the kinetic energy attained by the ions in the accelerator enables them to penetrate the surface, giving rise to a series of atomic displacements. These lattice-atom displacements tend to randomize distributions of alloying components until the energy is dissipated [1]. The technique thus leads to the modification of a small layer beneath the surface with a typical depth of 200 nm, producing an increase in hardness and resistance to wear, abrasion, high temperature oxidation and electrochemical corrosion [2–5]. Most studies have focused on improving the mechanical properties and high temperature resistance of alloyed steels and superalloys by nitrogen ion implantation and little work has been carried out on other materials such as copper.

It is well known that the oxidation and tarnishing of copper in industrial environments can reduce its conductivity, with a consequent loss of electrical properties. The need to increase the electrochemical and mechanical stability of copper contact interfaces has led to the use of gold or nickel–palladium coatings. An interesting alternative to this costly process is ion implantation. Hendriksen *et al.* [6] have studied the increase in corrosion resistance and surface microhardness of copper and silver electrical contacts resulting from boron ion implantation. More recently, Lambri *et al.* have studied some of the mechanical properties of nitrogen-implanted copper [7]. The literature also reports that the formation of nitrides on different metals by nitrogen ion implantation is very useful, providing great hardness, wear reduction, a gold colour and high corrosion resistance [8–10]. Following this line, the present paper focuses on the corrosion behaviour of copper surfaces modified by nitrogen ion implantation. Most of the experimental study was based on the application of impedance spectroscopy. This technique is a powerful tool for studying electrochemical systems such as ion-selective membranes [11], solid electrolytes [12], conducting polymers [12] and metallic corrosion [13]. The improvement in copper corrosion resistance after ion implantation makes these materials attractive due to their potential applications for the design of new contact materials for the electricity and electronic industries.

* Author to whom correspondence should be addressed.

0021-891X © 1997 Chapman & Hall

2. Experimental details

Pure copper specimens were prepared in the form of rectangular plates 15 mm long and 5 mm wide. Before the specimens were introduced into the implantation system their surfaces were treated in accordance with usual cleaning and polishing standards for industrial finishes.

The nitrogen ion implantation process was carried out using an industrial Wickham IBS generator, applying an acceleration voltage of 100 keV, a mean current of 0.40 mA and a nitrogen dosage of 4×10^{17} ions cm^{-2}. The specimens were cooled to prevent their temperature exceeding 40 °C during the 5 h of treatment.

Surface analyses of the specimens were carried out by Auger electron spectroscopy (AES) using a Perkin–Elmer ϕ 4200 Auger electron spectrometer and a Jeol (Jamp-S10) with a 5 kV electron source and a spot diameter of 100 μm. Argon ion etching for depth profiling was performed using an ion gun operating at 2 kV, which rastered an area of 2 mm × 2 mm. Profile Code™ software (Implant Science Corporation) was used to simulate nitrogen implantation conditions in the copper specimens. The parameters introduced in the simulation model were the same as for real implantation.

Most of the experimental study was based on the application of electrochemical impedance spectroscopy (EIS), though d.c. polarization resistance measurements were also made. All electrochemical measurements were performed with a three-electrode configuration. 0.6 M sodium chloride solutions were used as electrolyte. The surface area of the specimens exposed to the electrolyte was 0.75 cm^2. A platinum grid was used as counter electrode and a saturated calomel was used as reference electrode.

Electrochemical impedance measurements were made using an EG&G Princenton Applied Research (PAR) model 398 electrochemical impedance system with a 1255 Solartron frequency response analyser connected to a PARC 273A potentiostat/galvanostat. Some impedance data were collected with the Chiodelli interactive graphic program [14]. Impedance spectra were ranged from 10^5 to 10^{-3} Hz. The amplitude of the superimposed a.c. signal was 10 mV. The impedance data were fitted using the 'EQUIVCRT' program by Boukamp [15]. The d.c. polarization resistance (R_p) measurements were made with the PARC 273A potentiostat/galvanostat according to two different methods: one using a timed technique and the other using a scanning technique. Both d.c. techniques were carried out using the EG&G PAR model 352 analysis software. The timed (potentiostatic) technique was performed keeping the potential constant and plotting the resultant current against time. The potential steps applied were of ± 20 mV with respect to the corrosion potential and the step duration was 120 s. The scanning (linear polarization) technique was performed using a controlled-potential scan of ± 20 mV with respect to the corrosion potential and a scan rate of 0.166 mV s^{-1}.

3. Results and discussion

As can be seen in Fig. 1, surface analyses by Auger electron spectroscopy (AES) reveal that the as received specimens contain large amounts of surface contaminants like Cl, C, S, N and O. These specimens were cleaned by means of Ar$^+$ ion bombardment. After a few minutes of sputtering only small amounts of C and O were found (Fig. 1). At this point, ion implantation was begun.

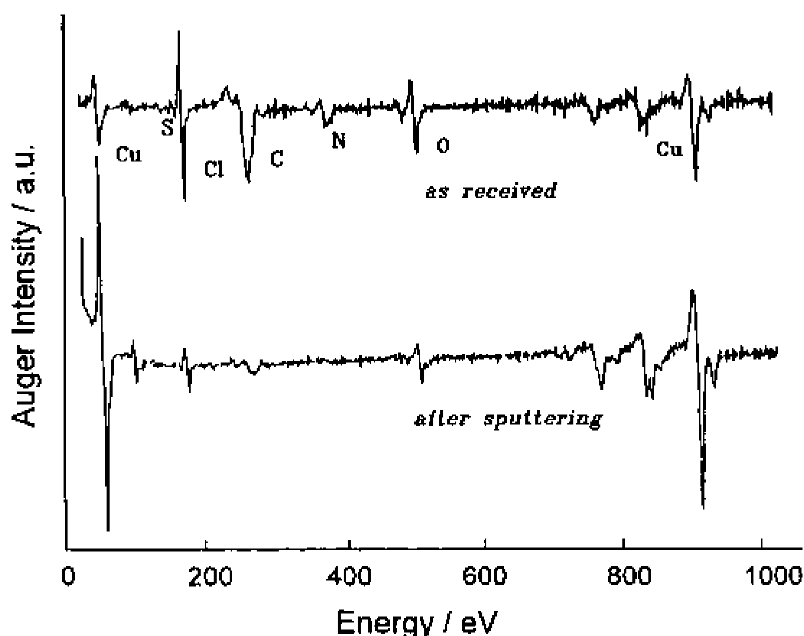

Fig. 1. Auger electron spectroscopy analyses of a nonimplanted copper specimen before and after the sputtering treatment.

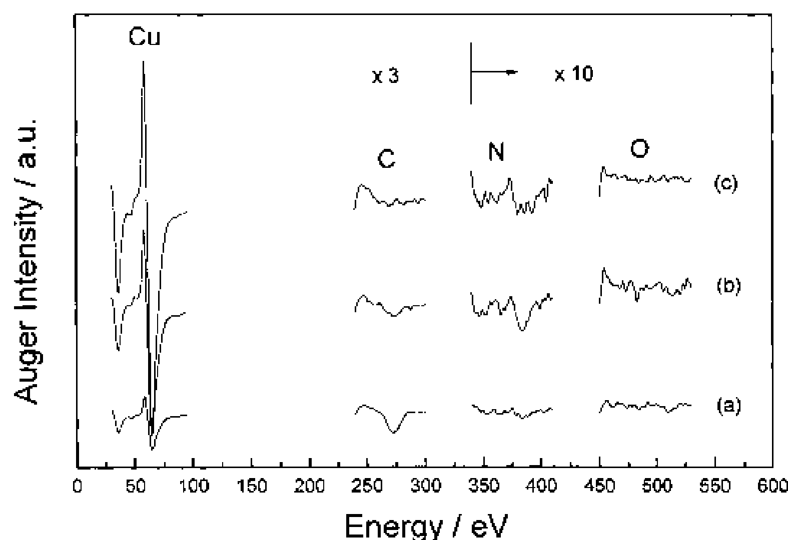

Fig. 2. Auger electron spectroscopy analyses of a nitrogen-implanted copper specimen, for different sputter depths: near the outer surface of the implantation layer (a) and increasing progressively the depths into the layer (b) and (c).

Figure 2 shows the Auger electron spectra corresponding to the Cu (LVV), C (KLL), N (KLL), and O (KLL) peaks at different depths of the sputter profile for a nitrogen ion-implanted specimen. AES scans were made only in particular spectrum regions, looking for these transitions. The Auger spectra reveal that there is no significant contamination of the copper surface by carbon during the implantation process. None of the nitrogen-implanted specimens presented greater oxygen content than the non-implanted specimens. A light sputtering with argon produces a progressive removal of oxygen and carbon beneath the outer surface of the implantation layer. The decrease in the C and O contents causes a change in the structure of the Cu (LVV) transition due to changes in the oxidation state of the copper (Fig. 2). At the same time, when the sputter depth increases, the Auger spectra show that there is an increase in the nitrogen content within the implantation layer (Fig. 2).

The nitrogen depth profiles obtained by simulation techniques are in agreement with these results. Figure 3 shows the nitrogen concentrations obtained using Profile Code^{TM} software. The parameters of the model are the same as for real implantation. The N profile has a Gaussian distribution. The maximum nitrogen concentration is 3.14×10^{22} ions cm^{-3} at 142.9 nm, and the maximum depth of copper bulk affected by nitrogen implantation is about 250 nm (Fig. 3).

The impedance (Nyquist) plots for the non-implanted specimens show a single semicircle in the frequency range studied (Fig. 4). This can be described with the equivalent circuit proposed in Fig. 4, where R_1 is the resistance of the electrolyte between the working electrode and reference electrode, R_2 is the charge transfer resistance at the metal/electrolyte interface, and CPE is a constant phase element. In many cases this impedance element was introduced formally only for fitting impedance data [15]. Nevertheless, the CPE behaviour has sometimes been ascribed to the fractal nature of the interface [16]. For a planar or smooth electrode, the nonfaradaic process may be represented by a classical double layer capa-

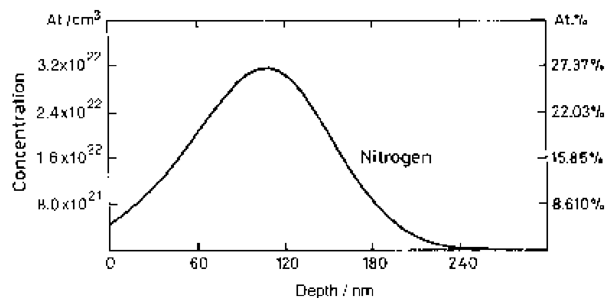

Fig. 3. Concentration profile of implanted nitrogen according to the theoretical model used for the simulation of the ion-implantation process.

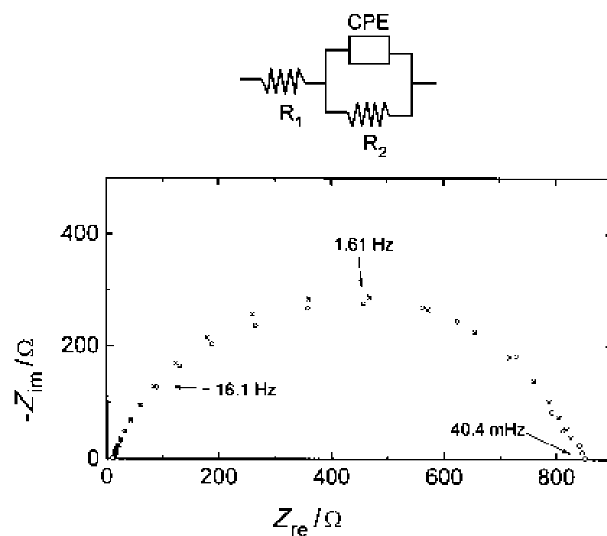

Fig. 4. Experimental (○) and simulated (×) Nyquist plots of a nonimplanted copper specimen. Immersion time: 3 d. Electrolyte: 0.6 M NaCl.

citance. However for a rough electrode such as these specimens, especially at high frequencies, the frequency dispersion of impedance is analogous to a nonuniform transmission line. Therefore such a nonfaradaic response can be represented by a more general constant phase angle element which is described by an empirical impedance function of the type:

$$Z(\omega) = 1/Y_0(\mathrm{j}\ \omega)^n$$

where j is the imaginary number ($\mathrm{j}^2 = -1$), Y_0 is the CPE constant ('S'), ω is the angular frequency (rad s^{-1}), $n = \alpha/(\pi/2)$ is the CPE power and, α is the phase angle of the CPE. The factor n is an adjustable parameter that usually lies between 0.5 and 1 [16]. The CPE only describes an ideal capacitor when $n = 1$. Otherwise, for $0.5 < n < 1$ the CPE describes a distribution of dielectric relaxation times in frequency space. Table 1 shows the variations with time for the values of the two CPE parameters, Y_0 and n. These values were obtained by fitting experimental and simulated data with the Boukamp program. The n values are between 0.70 and 0.76. Thus, the CPE describes a distribution of relaxation times [16].

Table 1. Changes in the impedance response of a nonimplanted copper specimen with immersion time in a 0.6 M NaCl electrolyte

Immersion time/ h	R_2 /Ω	*CPE* Y_0 / *'S'*	*n*
3	1100	7.58×10^{-5}	0.77
24	863	1.34×10^{-4}	0.76
48	860	2.02×10^{-4}	0.76
72	872	5.54×10^{-4}	0.69
96	889	6.36×10^{-4}	0.71
120	879	5.59×10^{-4}	0.70
144	860	2.39×10^{-4}	0.72
192	860	2.31×10^{-4}	0.71
360	856	2.19×10^{-4}	0.71

To simplify this discussion, it is useful to replace the CPE by the double layer capacitance, C. The approximate value of C is obtained from the equation

$$C = 1/(R_2\ \omega_{\max}) \qquad (1)$$

where R_2 values are given by the diameter of the single semicircles in the impedance diagram, and $\omega_{\max}$ is the angular frequency corresponding to the maximum of this semicircle. In the case of nonimplanted copper specimens C has a value of 3.6×10^{-4} F after three days of immersion in a 0.6 M NaCl solution (Fig. 4). This value does not correspond to the actual capacitance, but is useful for comparison with the values obtained for the nitrogen-implanted copper specimens.

Finally, in relation with the nonimplanted copper specimens, Table 1 also shows the changes with time for the R_2 values. In this case R_2 represents the charge transfer resistance of the corrosion reaction. These R_2 values are later used to calculate the corrosion rate of the material.

The impedance plots for the nitrogen-implanted specimens describe two clearly differentiated semicircles (Fig. 5). The problem is now to identify the impedance spectra region associated to the corrosion reaction of the metallic substrate. It should be remembered that an arc also appears at low frequencies when the diffusion layer has a finite thickness, and this arc may be confused with a semicircle, especially when data are not very precise [17]. In such a case, the high frequency semicircle is associated with the charge transfer resistance in the metal/electrolyte interface, while the low frequency arc is due to diffusive phenomena in the finite thickness layer. This situation may be described by incorporating a Warburg diffusion impedance in the finite length regime (Z_W) in the equivalent circuit, connected in parallel with the CPE and in series with R_2, respectively (Fig. 5). The impedance, Z_W, of the finite length element is defined by

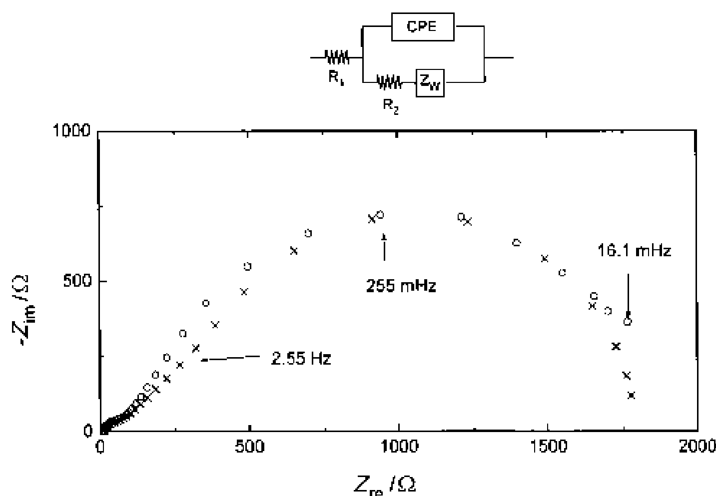

Fig. 5. Experimental (○) and simulated (×) Nyquist plots of a nitrogen-implanted copper specimen. Immersion time: 3 d. Electrolyte: 0.6 M NaCl.

$$Z_W = \tanh\,[B\,(j\omega)^{1/2}]\;/\;Y_0\,(j\omega)^{1/2}$$

where Y_0 and B contain the diffusion coefficient and other material constants [15].

However, if the diffusion model is accepted, the calculated values for the elements in this equivalent circuit give high relative errors when the nonlinear least squares fit technique of the Boukamp computer program is used (Table 2). On the other hand, the capacitance values of the low frequency arc, derived from the expression

$$C_2 = 1/(R_3\,\omega_{\max}) \tag{2}$$

have the same order of magnitude as those of the single semicircle obtained for nonimplanted specimens. Thus, for instance, $C_2 = 3.20 \times 10^{-4}$ F for three days of exposure to the electrolyte (Fig. 5). Moreover, these results contradict those found for the low frequency arc associated with curved diffusion lines, where the values of capacitance (pseudocapacitance) derived from Expression 2 are usually higher than the values obtained in the present case [18, 19]. All these results indicate that yet it is necessary to look for other equivalent circuits in order to give a physical interpretation more satisfactory for the impedance plots found for the nitogen-implanted specimens.

The protective layers produced during the ion implantation process are thin and have a little compactness or continuity and may therefore cause the development of cathodic and anodic areas on the electrode. Using surface analyses and depth profiling, Zhang *et al.* [20] have shown the importance of the spatial distribution of implanted ions and, the effect of these ions on the development of anodic and cathodic areas on the metal surface, during the corrosion reaction of specimens prepared by ion implantation of Cr, Ni and W in Pb and Pb–4%Sb. In this way, it could be of interest to use the equivalent circuit proposed by Keddam *et al.* (Fig. 6(a)) [21] to study the influence of the presence of these cathodic and anodic areas on the specimen. However, nonlinear least squares fit (NLLS-fit) techniques do not give good results with this equivalent circuit when applied to experimental data of nitrogen-implanted specimens, and the relative errors found for the values of the elements of the equivalent circuit are unacceptable (Table 2).

Two other equivalent circuits may be proposed, both with two relaxation time constants (Fig. 6(b) and (c)). These electrical circuits are typically used in studies of ion-selective membranes [22, 23], when examining metallic corrosion under organic coatings [24–27], in certain instances of localized corrosion

Table 2. Results obtained applying the NLLS-fit technique to the experimental impedance data of a nitrogen-implanted copper specimen, after three days immersed in a 0.6 M NaCl solution, using different equivalent circuits

Equivalent circuit	*CDC**	*Element circuit*	*Value*	*Relative error/%*
Fig. 5	$R_1(Q[R_2O])$	R_1	9.92 Ω	8.80
		Q–Y_0	2.08×10^{-5} ‘S’	79.49
		Q–n	0.79	10.05
		R_2	5.66×10^{1} Ω	24.14
		O–Y_0	7.92×10^{-4} ‘S’	3.86
		O–B	$1.36\ s^{1/2}$	5.54
Fig. 6(a)	$([R_1(Q_1R_2)][R_3(Q_2R_4)])$	R_1	1.01×10^{1} Ω	–
		Q_1–Y_0	4.77×10^{-5} ‘S’	–
		Q_1–n	0.70	6.20
		R_2	2.36×10^{3} Ω	–
		R_3	1.25×10^{2} Ω	–
		Q_2–Y_0	3.49×10^{-4} ‘S’	–
		Q_2–n	0.74	4.33
		R_4	1.58×10^{4} Ω	–
Fig. 6(b)	$R_1(R_2Q_1)(R_3Q_2)$	R_1	9.33 Ω	7.10
		R_2	9.08×10^{1} Ω	12.39
		Q_1–Y_0	6.36×10^{-5} ‘S’	36.09
		Q_1–n	0.69	5.82
		R_3	1.95×10^{3} Ω	5.59
		Q_2–Y_0	4.29×10^{-4} ‘S’	6.29
		Q_2–n	0.74	3.95
Fig. 6(c)	$R_1(Q_1[R_2(Q_2R_3)])$	R_1	9.37 Ω	7.35
		Q_1–Y_0	5.57×10^{-5} ‘S’	40.51
		Q_1–n	0.70	6.15
		R_2	1.11×10^{2} Ω	13.76
		Q_2–Y_0	3.80×10^{-4} ‘S’	9.90
		Q_2–n	0.74	4.35
		R_3	1.95×10^{3} Ω	5.51

* CDC is the circuit description code according to the Boukamp program

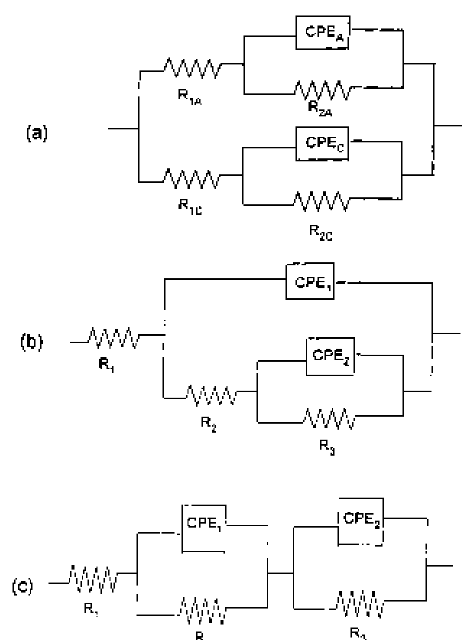

Fig. 6. Some equivalent circuit models that yield impedance spectra with two relaxation time constants.

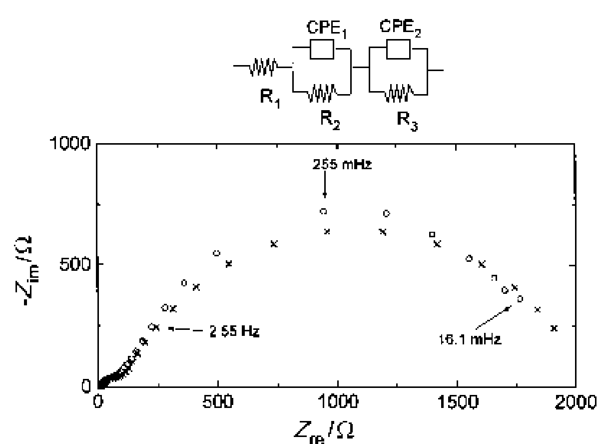

Fig. 7. Experimental (○) and simulated (×) Nyquist plots of a nitrogen-implanted copper specimen. Immersion time: 3 d. Electrolyte: 0.6 M NaCl. (Simulated data are obtained with a different equivalent circuit to that shown in Fig. 5).

[28], and systems where surface layers may form during exposure to a corrosive environment [29]. Both equivalent circuits give successful results with NLLS-fit techniques when applied to the study of the impedance response of the nitrogen-implanted specimens (Table 2).

Figure 7 shows experimental and simulated impedance plots obtained after three days of exposure in a 0.6 M NaCl solution. Table 3 shows the changes with time for the parameters Y_0 and n for both constant phase elements CPE_1 and CPE_2, of the nitrogen-implanted specimens. These values were calculated using the equivalent circuit in Fig. 6(c). It may be observed that the CPE_2–Y_0 values in the low frequency semicircle are of the same order of magnitude as those found for parameter Y_0 which correspond to the single semicircle of the impedance plots for nonimplanted copper specimens (Table 1). These results indicate that the low frequency semicircle for the nitrogen-implanted copper specimens has the same meaning as the single semicircle that appears for nonimplanted specimens. Thus, this low frequency semicircle may be associated with the charge transfer of the corrosion reaction of the metallic substrate.

Finally, the behaviour of the impedance response of the nitrogen-implanted specimens at high frequencies suggests that the element R_2 in the equivalent circuit proposed in Fig. 6(c) represents to the ionic resistance of the protective layer developed in the copper surface as a result of the implantation process, and CPE_1 is related to the dielectric properties of this layer [13].

Fujihana *et al.* [30] have observed that the nitrogen ion implantation in chromium films leads to the formation of chromium nitride layers and improves the corrosion resistance of these materials. Some authors have also observed the formation of an oxide layer on freshly nitrogen-implanted metal surfaces during exposure to the atmosphere [3, 31]. This oxide film was not dense but had a greater thickness on implanted surfaces than on nonimplanted surfaces improving the corrosion resistance of the nitrogen-implanted materials [31]. In the case of the nitrogen-implanted copper specimens the AES analyses show that copper nitrides may have a greater influence than copper

Table 3. Changes in the low (a) and high frequency (b) impedance responses of a nitrogen-implanted copper specimen with immersion time in a 0.6 M NaCl electrolyte

	(a) *High frequency semicircle*			(b) *Low frequency semicircle*		
Immersion time/h	R_2 /Ω	CPE_1 Y_{01} / 'S'	n_1	R_3 /Ω	CPE_1 Y_{02} / 'S'	n_2
3	15600	2.40×10^{-7}	0.77	2200	2.70×10^{-4}	0.78
24	7200	6.80×10^{-7}	0.76	2000	3.91×10^{-4}	0.76
48	1420	2.90×10^{-6}	0.76	1950	4.10×10^{-4}	0.76
72	90.8	6.35×10^{-5}	0.69	1953	4.29×10^{-4}	0.74
96	95.5	5.03×10^{-5}	0.71	1890	4.08×10^{-4}	0.76
120	90.5	5.60×10^{-5}	0.70	1725	6.20×10^{-4}	0.76
144	–	–	–	1700	5.90×10^{-4}	0.77
192	–	–	–	1710	6.10×10^{-4}	0.76
360	–	–	–	1710	6.15×10^{-4}	0.80

oxides on the electrochemical behaviour of these specimens, in view of the low oxygen content found in the ion implantation layer (Fig. 2).

The copper nitride formed during the implantation process will constitute a protective barrier to the anodic dissolution process of the metallic substrate, this being important for delaying the corrosion. Nevertheless, the high capacitance values calculated from these Nyquist plots ($C_l = 10^{-6}$–10^{-8} F) indicate that this protective layer is neither continuous nor compact. In fact, the results of the theoretical depth profile model showed previously that the atomic concentration of implanted nitrogen was less than 9% for depths greater than 180 nm (Fig. 3). The thinness of this protective layer is not sufficient to obtain a continuous film, but may be enough to improve the corrosion resistance of the modified copper surface, as will be shown below.

The intersection point of the low frequency semicircle on the real axis for $\omega \rightarrow 0$ is an important constituent of the Nyquist plot. In general, the value of this intersection point may be used to obtain the apparent a.c. polarization resistance, R_p. Thus, for instance, for an exposure to the electrolyte of 3 h, the a.c. R_p value of 17 837 Ω for nitrogen-implanted specimens and 1109 Ω for nonimplanted copper specimens.

Alternatively, Fig. 8 shows a potentiostatic plot in which the variations in the response current are represented against time for a 20 mV cathodic potential step. The ratio between the applied potential and the response current was used to obtain the d.c. apparent polarization resistance values when the steady state is reached. Except when measurements are made under conditions far from the steady state, the apparent d.c. R_p values obtained from the potentiostatic technique virtually coincide with the apparent a.c. R_p values [32]. In the case of the nitrogen-implanted copper specimens, the results obtained with both techniques coincide.

Figure 9 shows some results of the other d.c. electrochemical technique applied to measure linear polarization. In the case, the resultant current was plotted against the potential using logarithmic scale. The R_p was determined using a linear least-squares fit of data which is included in the model 352 software package. The apparent d.c. R_p values obtained with this technique agree again with those obtained with the electrochemical impedance technique (EIS), presenting the same order of magnitude and similar evolution with immersion time as those obtained with EIS.

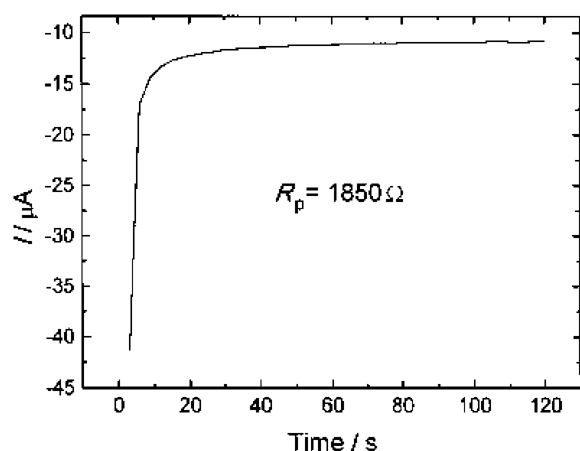

Fig. 8. Current–time response versus a 20 mV potential step for a nitrogen-implanted copper specimen. Time setup: 2 min. Immersion time: 15 d. Electrolyte: 0.6 M NaCl.

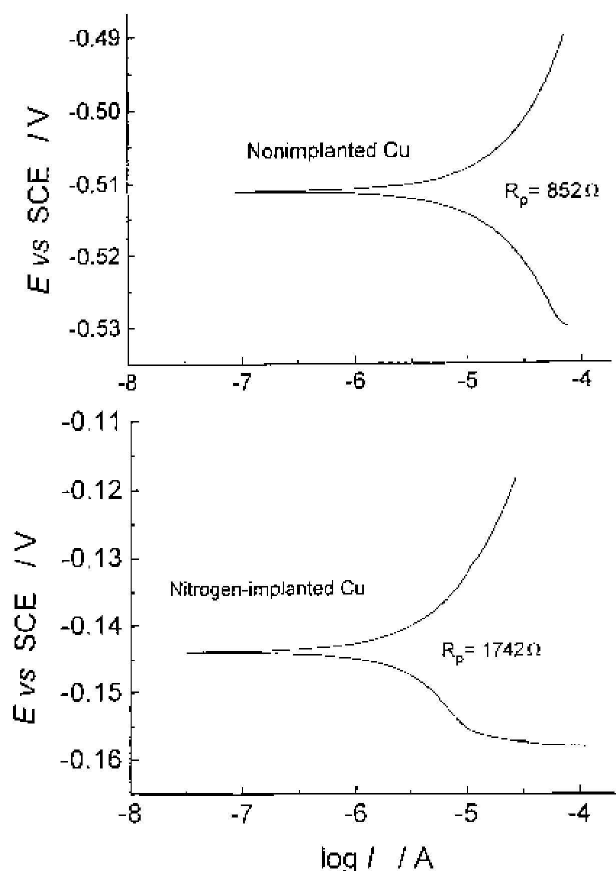

Fig. 9. Linear polarization plots for nitrogen-implanted and nonimplanted copper specimens, respectively. Immersion time: 8 d. Electrolyte: 0.6 M NaCl.

Once the apparent R_p is known, the corrosion rate may be calculated using the Stern–Geary equation ($i_{corr} = B/R_pS$) [33], in order to obtain kinetic information about the corrosion process. For this purpose, it may be assumed a B value of 0.026 V, which is very commonly used [34]. Table 4 shows the variations in the corrosion rate with the immersion time, for both nonimplanted and nitrogen-implanted copper specimens, respectively, in a 0.6 M NaCl solution. It may be observed that the i_{corr} values for nitrogen-implanted specimens are always lower than for nonimplanted copper specimens, especially during the first 48 h of exposure to the electrolyte.

All these results indicate that the modification of copper surfaces by nitrogen ion implantation improves the corrosion resistance of the as received materials, although it would be necessary to optimize some parameters of the ion implantation treatment in order to further reduce the corrosion rate and improve the corrosion resistance of these materials.

Table 4. Variations of the corrosion rate (i_{corr}) with the immersion time, for nonimplanted and nitrogen-implanted copper specimens in a 0.6 M NaCl solution

Exposure time / h	*Nonimplanted specimens* i_{corr} / μA cm^{-2}	*Nitrogen implanted specimens* i_{corr} / μA cm^{-2}
3	31.6	2.0
24	40.2	3.9
48	40.3	10.3
72	39.8	17.0
96	39.0	17.5
120	39.4	19.1
144	40.3	20.4
192	40.3	20.3
360	40.5	20.3

4. Conclusions

The electrochemical impedance spectroscopy has been very useful for investigating both mechanism and kinetic aspects related to the corrosion processes developed on copper surfaces modified by nitrogen ion implantation.

For the nonimplanted copper specimens, the impedance plots show a single semicircle which may be ascribed to a charge transfer control of the corrosion reaction which takes place on the metal surface. Alternatively, the form of the Nyquist plots obtained for the nitrogen-implanted specimens could indicate that a mixed control (activation plus diffusion) takes place during the corrosion process of these specimens. Nevertheless, the parameter values obtained from these impedance plots indicate that the high frequency semicircle that appears in these plots is associated with the protective properties of the surface layer formed during the ion implantation process, while the low frequencies semicircle has the same physical meaning as the single semicircle appearing for the nonimplanted specimens.

With regard to kinetic aspects, impedance spectroscopy and other electrochemical techniques applied in this study (potentiostatic and linear polarization methods) show that the apparent corrosion rate for the implanted specimens is always lower than for the nonimplanted copper specimens.

All of these results confirm that the surface modification by nitrogen ion implantation of copper forms a protective surface layer which improves the corrosion resistance of the as received material, a feature of great interest for the design of new contact materials for the electricity and electronic industries.

Acknowledgements

Financial support from the CICYT under contract number MAT 93-0630-C02 is gratefully acknowledged. AIN also thanks Iberdrola for supporting part of its research. Authors also acknowledge Dr Mercedes F. Rodríguez (Instituto de Ciencia de Materiales de Madrid) for performing some of the AES analyses.

References

[1] L. Rehn, S. T. Picraux and H. Wiedersich, *in* 'Surface Alloying by Ion, Electron and Laser beam' (edited by L. Rehn, S. T. Picraux and H. Wiedersich), ASM, Ohio (1987), pp. 1–17.

[2] C. H. Yang, G. Welsch and T. E. Mitchell, *J. Mater. Sci.* **25** (1990) 1724.

[3] M. Nikolova, K. Takahashi and M. Iwaki, *J. Appl. Electrochem.* **24** (1994) 52.

[4] R. D. Granata, M. A. De Crosta, J. F. McIntyre and H. Leidheiser, Jr., *Ind. Eng. Chem. Res.* **26** (1987) 427.

[5] P. Mazzoldi, *in* 'Advanced Techniques for Surface Engineering' (edited by W. Gissler and H. Jehn Kluwer), Academic, Dordrecht (1992), p. 83.

[6] O. Henriksen, E. Johnson, A. Johansen, I. Sarholt-Kristensen and J. Wood, *Nucl. Instrum. & Methods Phys. Res.* 19/20 (1987) 253.

[7] O. A. Lambri, G. Sanchez, J. Feugeas, and F. Povolo, *Surf. Coat. Technol.* **70** (1–2) (1995) 191.

[8] K. Takahashi, *J. Met. Finish. Soc. Jpn* **39** (1988) 579.

[9] K. Terashima *et al.*, International Conference on 'Surface Modification of Metals by Ion Beams', Kingston, Ontario, 1986, *Mater. Sci. Eng.* **90** (1987) 229; *Surf. Eng.* **4** (1988) 90.

[10] E. Leitao, C. Sa, R. A. Silva, M. A. Barbosa and H. Ali, *Corros. Sci.* **37** (1995) 1861.

[11] (a) P. Aranda, A. Jimenez-Morales, J. C. Galván, B. Casal and E. Ruiz-Hitzky, *J. Mater. Chem.* **5** (1995) 817; (b) J. C. Galván, P. Aranda, J. M. Amarilla, B. Casal and E. Ruiz-Hitzky, *ibid.* **3** (1993) 667.

[12] (a) E. Ruiz-Hitzky, P. Aranda, B. Casal and J. C. Galván, *Adv. Mater.* **7** (1995) 180; (b) E. Ruiz-Hitzky, *ibid.* **5** (1993) 334.

[13] J. R. Macdonald (ed.), 'Impedence Spectroscopy; Emphasizing Solid Materials and Systems', Wiley & Sons, New York (1987).

[14] (a) G. Chiodelli, 'Interactive Graphic Programs for F.R.A. Solartron 1255/1260 (V92)', CSTE-CNR / Universita' di Pavia; (b) G. Chiodelli and P. Lupotto, *J. Electrochem. Soc.* **138** (1991) 2703.

[15] (a) B. A. Boukamp, 'Equivalent Circuit' (EQUIVCRT.-PAS), version 4.51. University of Twente, (1989); (b) B. A. Boukamp, *Solid State Ionics* **20** (1986) 31.

[16] U. Rammelt and G. Reinhard, *Electrochim. Acta* **35** (1990) 1045.

[17] S. Feliu, J. C. Galván and M. Morcillo, *Prog. Organic Coatings* **17** (1989) 143.

[18] J. C. Galván, S. Feliu and M. Morcillo, *ibid.* **17** (1989) 135.

[19] S. Feliu, J. C. Galván and M. Morcillo, *Corros. Sci.* **30** (1990) 989.

[20] S. T. Zhang, F. P. Kong and R. H. Muller, *J. Electrochem. Soc.* **141** (1994) 2677.

[21] M. Keddam, X. R. Novoa, L. Soler, C. Andrade and H. Takenouti, *Corros. Sci.* **36** (1994) 1155.

[22] P. Aranda, J. C. Galván, B. Casal and E. Ruiz-Hitzky, *Colloid Polym. Sci.* **272** (1994) 712.

[23] R. D. Armstrong, A. K. Covington and G. P. Evans, *J.Electroanal. Chem.* **159** (1983) 33.

[24] I. Thompson and D. Campbell. *Corros. Sci.* **37** (1995) 67.

[25] A. Miszczyk and H. Szalinska, *Prog.Organic Coatings* **25** (1995) 357.

[26] F. Deflorian, L. Fedrizzi and P. L. Bonora, *ibid.* **23** (1–4) (1993) 73.

[27] R. D. Armstrong and D. Wright, *Electrochim. Acta* **38** (1993) 1799.

[28] R. Oltra and M. Keddam, *Corr. Sci.* **28** (1988) 1.

[29] D. C. Silverman, *Corrosion* **46** (1990) 589.

[30] T. Fujihana, N. Matsuzawa, Y. Okabe and M. Iwaki, Proceedings of the 3rd Symposium on 'Surface Layer Modifiction by Ion Implantation', Ionics Publishers, Tokio (1987), p. 45.

[31] V. Ashworth, W. A. Grant, R. P. M. Procter and T. C. Wellington, *Corros. Sci.* **16** (1976) 393.

[32] J. C. Galván, S. Feliu Jr., M. Morcillo, J. M. Bastidas, E. Almeida, J. Simancas and S. Feliu, *Electrochim. Acta* **37** (1992) 1983.

[33] M. Stern and A. L. Geary, *J. Electrochem. Soc.* **104** (1957) 56.

[34] L. M. Callow. J. A. Richardson and J. L. Dawson, *Bri. Corros. J.* **11** (1976) 123.